Novel Geometric Representation for One-Dimensional Model of Arterial Blood Pulse Wave Propagation

Prashanth Ramakrishna, Nabeel P M, *Member, IEEE*, and Mohanasankar Sivaprakasam

***Abstract*— This paper proposes a novel one-dimensional graphical representation to model the phenomenon of blood pulse wave propagation in major arteries. In particular, a tree data structure, as opposed to the existing purely linear structures, is used to accommodate arterial branching. The model is qualitatively validated and demonstrated its reliability by evaluating the phenomenon of wave reflection and pulse pressure amplification with a sample *in-vivo* arterial segment length measurements.**

I. Introduction

Blood pressure is critical in accurately characterizing cardiovascular diseases and correctly diagnosing patients with such diseases in clinical settings. Measured blood pulse pressure waves, however, are a generated by a complex system of arterial blood propagation that cannot be investigated through simple pressure-band measurement, which is known to be extremely error prone [1]. Mathematical modeling of blood pulse pressure wave propagation through the arterial system has therefore become increasingly important in extracting important diagnostic information, such as arterial distensibility. One constituent phenomenon of blood pressure for which there remains inadequate modelling is blood pulse wave reflection, specifically at arterial bifurcations [2] Typically, wave reflections have been modeled without consideration of the vessel bifurcation pattern, the primary producer of wave reflections, by using one-dimensional (1D) geometric representations of inter-branching arterial segments. In such representations, reflections are caused by any sort of irregularities or biomechanical impedance mismatch between the vessel segments. At these irregularities the incident wave is split into two components, one forward moving and the other backward moving. This process is described by *transmission* and *reflection* coefficients, dictating how the incident wave is separated. The measured wave form can be determined by storing the coefficients of each wave split as a wave *propagation history* [3], [4]. Such a representation, however, is insufficient for modeling the full arterial system, and, further, does not lend itself to efficient algorithms for traversing propagation histories.

In this work, we present a full description the novel geometric tree representation of the arterial system, detailing how propagation history is stored as well as the proposed algorithm for determining effective reflected waves. Next, results are given, both using a simplified full binary tree and using a more realistic tree generated from in-vivo arterial segment. Finally, the limitations of this model are discussed as well as directions for further research on its basis.

Prashanth Ramakrishna is with the Department of Mathematics, New York University, NY 10009 USA (e-mail: pmr347@nyu.edu).

Nabeel P M is with the Department of Electrical Engineering, Indian Institute of Technology Madras (IIT Madras), Chennai, India.

Mohanasankar Sivaprakasam is with the Department of Electrical Engineering and the Director of Healthcare Technology Innovation Centre, Indian Institute of Technology Madras, Chennai, India.

II. Model Exposition

If one only considers an arterial segment in which impedance mismatches and, by extension, wave reflections are produced by irregularities such as aneurisms or stenosis and not by branching, then the resulting model will be characterized by a graphical representation as in Fig. 1.

Using this representation when bifurcations are absent is convenient because there is only a single path that can be taken to the system's final irregularity. Storing a propagation history of reflection and transmission coefficients can easily be done using matrices, despite the updating process for such matrices as irregularities are added to the system can become cumbersome. However, once bifurcations are introduced, this representation becomes untenable, since it allows for only a single transmitted wave at each impedance mismatch when, in reality, there may be multiple. We see that even modifying Fig. 1, as in Fig. 2, to accommodate bifurcations yields a representation, again, that is untenable due to the multiple final irregularities in the system all with unique paths originating at its entry point that make matrix storage of a propagation history impossible.

Therefore, it is necessary to develop an arterial representation that accommodates bifurcations without sacrificing the ability to efficiently traverse the system's propagation history. Intuitively, a tree representation seems an ideal fit. Not only does it work as a complete abstract structural analog to the arterial system, it also functions simultaneously as the data structure storing a traversable propagation history.

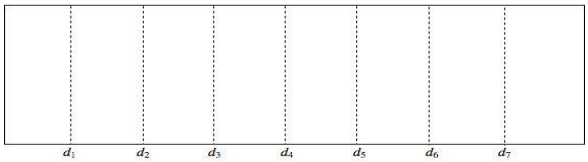

Figure 1. Typical 1D linear geometric representation of arterial segment.

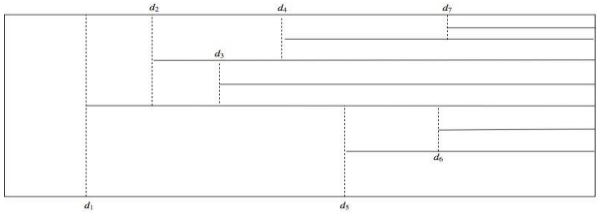

Figure 2. A sample of 1D linear geometric representation of arterial segment modified to accommodate arterial branching.

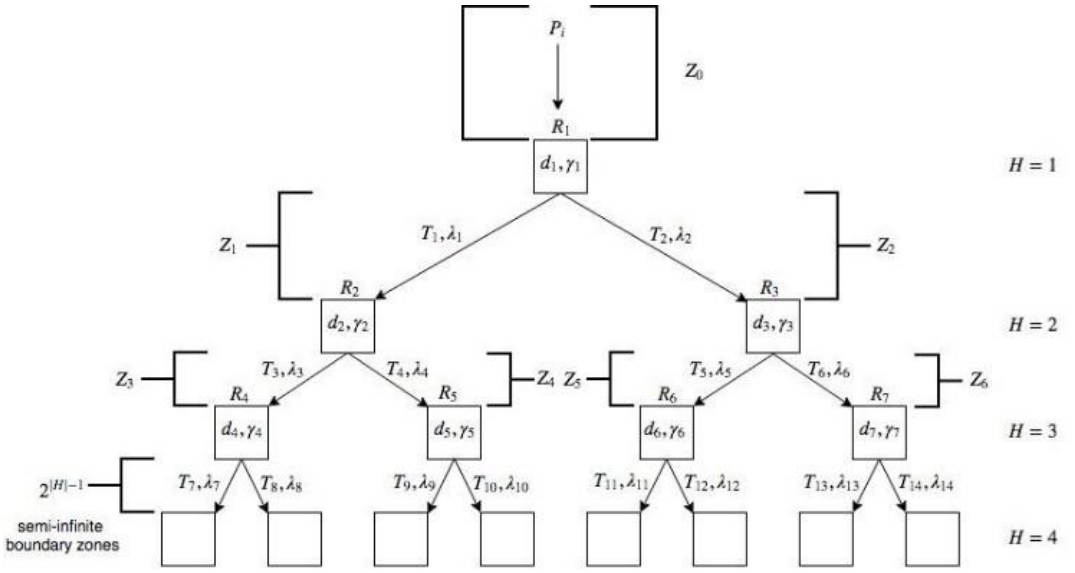

Figure 3. Geometric tree representation of arterial system with seven branchings S_7.

A. *Propagation History*

The general form of the system detailed in Fig. 3 is S_n, with n branchings indexed $\{d_1, d_2, \dots, d_n\}$. Between each branching is a physiologically homogenous zone, in which traveling waves are not perturbed in any way. These zones are denoted $\{Z_0, Z_1, \dots, Z_{2^{|H|}}\}$, where H is the height of the tree, and Z_0 and $\{Z_{2^{|H|-1}}, \dots, Z_{2^{|H|}}\}$ are semi-infinite boundary regions in which either the incident pulse wave P_i fed into S_n or the finally transmitted waves $\{T_{2^{|H|-1}+1}, \dots, T_{2^{|H|}}\}$ exit S_n.

Supposing an arterial scheme that maps to a fully binary tree (although this is not necessary), when a forward moving pulse T_{k-1}, transmitted through Z_{k-1}, meets branching d_k, it splits into three separate waves: two transmitted waves indexed T_{2k-1} and T_{2k} that travel forward through zones Z_{2k-1} and Z_{2k} respectively, and one reflected wave, R_{k+1}that propagates backwards through zone Z_{k-1}. The components into which an incoming wave is separated upon meeting a branching are characterized by the ratio of their amplitudes to the amplitude of their "parent" wave. These two ratios related to forward-moving components are known *transmission coefficients*, denoted λ_k and stored as the weight either of edge (d_k, d_{k+1}) or (d_{k-1}, d_{k+1}), and the ratio related to the one backward-moving component is known as the *reflection coefficient*, denoted γ_k and stored at node d_k. we thus have:

$$\gamma_k = \frac{A(R_k)}{A(T_{k-1})} \tag{1}$$

$$\lambda_{2k-1} = \frac{A(T_{2k-1})}{A(T_{k-1})} \tag{2}$$

$$\lambda_{2k} = \frac{A(T_{2k})}{A(T_{k-1})} \tag{3}$$

Where, $k \in [1, n]$, A returns the amplitude of its argument wave, and $\gamma_k + \lambda_{2k-1} + \lambda_{2k} = 1$.

B. *Computing Reflected Waves*

Not only is the geometric modeling of arterial branching as a tree very natural, it is also very efficient, since it makes available a host of very powerful recursive traversal algorithms that can be used to find the amplitude of any given reflected wave R_k given the stored propagation history. In turn, determining individual reflected waves allows the computation of the effective reflective wave R_E produced by S_n after P_i has passed through.

Note that $A(R_k)$ is given by $A(T_{k-1}) \times \gamma_k$. More specifically, this means that $A(R_k)$ is the product of $A(P_i)$, the transmission coefficients along the path to d_k (not including λ_k), and γ_k. Representing λ_k alternatively as the edge to which it belongs, either (d_k, d_{k+1}) or (d_{k-1}, d_{k+1}), the amplitudes for each reflected wave produced by the system shown in S_7 (Fig. 3) are:

H = 1:

$$A(R_1) = A(P_i) \times \gamma_1$$

H = 2:

$$A(R_2) = A(P_i) \times (d_1, d_2) \times \gamma_2$$
$$A(R_3) = A(P_i) \times (d_1, d_3) \times \gamma_3$$

H = 3:

$$A(R_4) = A(P_i) \times (d_1, d_2) \times (d_2, d_4) \times \gamma_4$$
$$A(R_5) = A(P_i) \times (d_1, d_2) \times (d_2, d_5) \times \gamma_5$$
$$A(R_6) = A(P_i) \times (d_1, d_3) \times (d_3, d_6) \times \gamma_6$$
$$A(R_7) = A(P_i) \times (d_1, d_3) \times (d_3, d_7) \times \gamma_7$$

Generally, we have

$$A(R_k) = A(P_i) \times \left(\prod_{\forall (i,j) \in p} (d_i, d_j)\right) \times \gamma_k, \tag{4}$$

where i and j are indices of adjacent nodes along the unique path p to d_{k-1}. Further, since the effective reflective wave R_E is given by

$$A(R_E) = \sum_{k=1}^{n} A(R_k), \tag{5}$$

R_E can finally be characterized as:

$$A(R_E) = A(P_i) \sum_{k=1}^{n} \gamma_k \prod_{\forall (i,j) \in p} (d_i, d_j). \tag{6}$$

Further, we can calculate the time at which each reflected wave is generated, T_g and the time at which each reflected wave returns to the point of measurement (mouth of S_n), T_m:

$$T_g(R_k) = \frac{1}{c}\sum_{u=1}^{k-1} l_u \quad (7)$$

$$T_m(R_k) = 2 \times T_g(R_k) \quad (8)$$

Where l_u represents the associated length of zone Z_u and c represents the speed of the incident wave P_i.

III. Validation Study Results

A. Validation with Sample System

For initial validation of this model, we first consider the system S_7 depicted in Fig. 3. We let P_i be a positive half-sine function with $A(P_i)$ = 30 from 80 to 110 mmHg, roughly approximating the pulsatile form of a blood pulse pressure wave. The period of P_i is 800 ms. Zone lengths are randomly drawn from a uniform distribution between 50 and 180 mm. Finally, reflection coefficients at each impedance mismatch are randomly drawn from a uniform distribution between 0.1 and 0.3.

In Fig. 4, we see the individual reflected waves generated in S_7. Each wave is subject to a phase shift depending on the time at which it was generated. Notice that the reflection waves reduce proportionally with each subsequent tree level. This is because the reflection coefficients for distal branchings are similar to those of proximal branchings. In reality though, as we move toward the periphery of the arterial system, impedance mismatches become greater and, by extension, so do reflection coefficients.

In Fig. 5 we have qualitative validation of the geometric tree representation. We observe a dicrotic notch as well the effects of minor pulse wave amplification. The pulse wave amplification here, though, is far less than would be measured *in-vivo*, where systole is amplified from between 100 and 110 to between 120 and 130. Further, the amplitude of the effective reflected wave shown in Fig. 5 has an amplitude of 15. This is very near to the usually observed amplitude of effective reflected waves, which is 50% of $A(P_i)$ [1], [2], [5].

B. Validation with In-vivo Data

Now that qualitative validation of the geometric tree representation has been established. We consider more realistic model parameters paired with *in-vivo* arterial segment measurement, aiming to produce more realistic, although still approximate, waveforms.

We construct a tree representation from the arterial scheme shown in Fig. 6. All arterial segments that do not lead to branching sites are excluded from the representation. This is because no reflection waves (according to this scheme) will propagate backwards through these segments and contribute to the effective reflected wave. This process is similar to excluding the leaves at $H = 4$ of S_7 in the calculation of R_E using (6).

Ultimately, the segments used are 3 (Brachiocephalic, 34 mm), 4 (Subclavian A, 34 mm), 7 (Subclavian B, 422 mm), 9 (Ulnar A, 67 mm), 19 (Subclavian A, 34 mm), 21 (Subclavian B, 422 mm), 23 (Ulnar A, 67 mm), 27 – 41 (Thoracic aorta B – Abdominal aorta E treated as single segment, 684 mm), 42 (Common iliac, 59 mm), 43 (Common iliac, 59 mm), 44 (External iliac, 144 mm), 46 (Femoral, 443 mm), 50 (External iliac, 144 mm), and 52 (Femoral, 443 mm) [6].

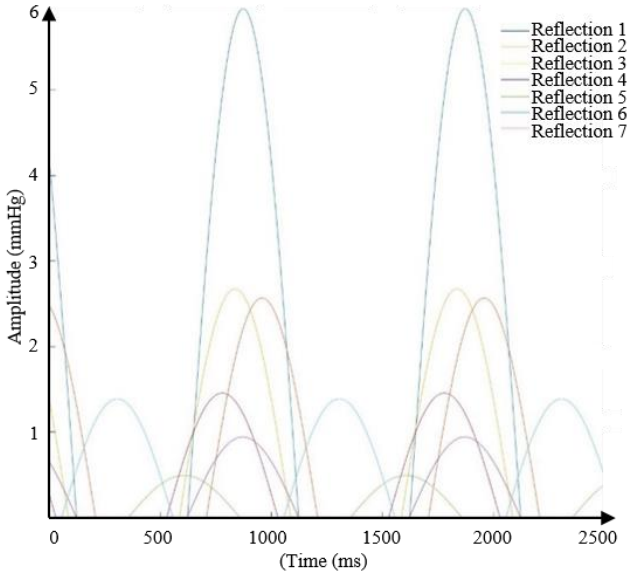

Figure 4. Individual reflected waves generated at each branching site in S_7.

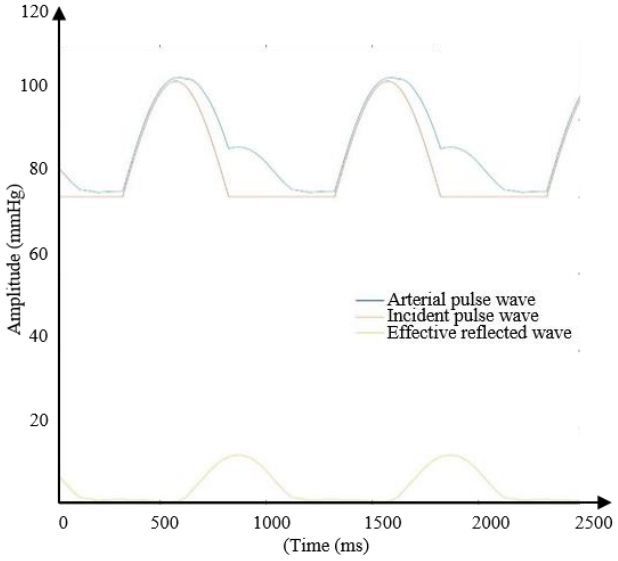

Figure 5. Summing $\mathbf{R_E}$ and $\mathbf{P_i}$ gives the final measured waveform.

In Fig. 7, the right branch corresponds to the portion of Fig. 6 stemming from the thoracic aorta, the middle branch corresponds to the portion stemming from the subclavian A, and the left branch corresponds to the portion stemming from the brachiocephalic. Each edge is characterized by a transmission coefficient and each node by a reflection coefficient. By storing these coefficients, the tree also stores the system's propagation history.

Notice in Fig. 8 that reflection coefficients are chosen randomly from uniform distributions of ascending ranges for subsequent tree levels. The greatest reflection coefficients are found at the periphery of the arterial system, where impedance mismatches are the greatest.

Summing R_E and P_i gives the final measured waveform using *in-vivo* arterial segment measurements. Note that the more uneven form of R_E is a result of a non-full non-binary tree structure, producing a greater range of reflected wave phase mismatches.

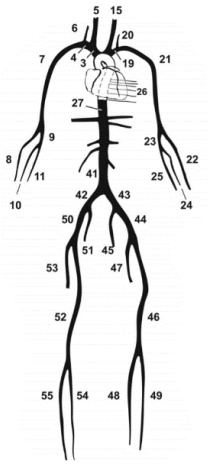

Figure 6. Fig 6: Full depiction of an arterial scheme [6].

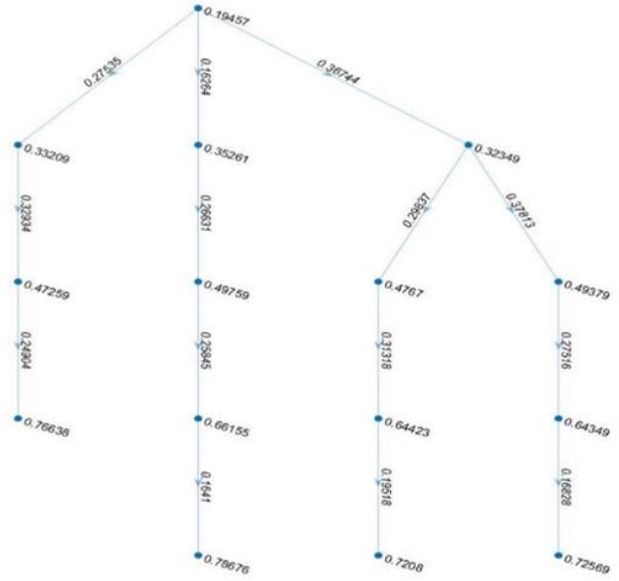

Figure 7. Tree representation constructed from arterial scheme in Fig. 6.

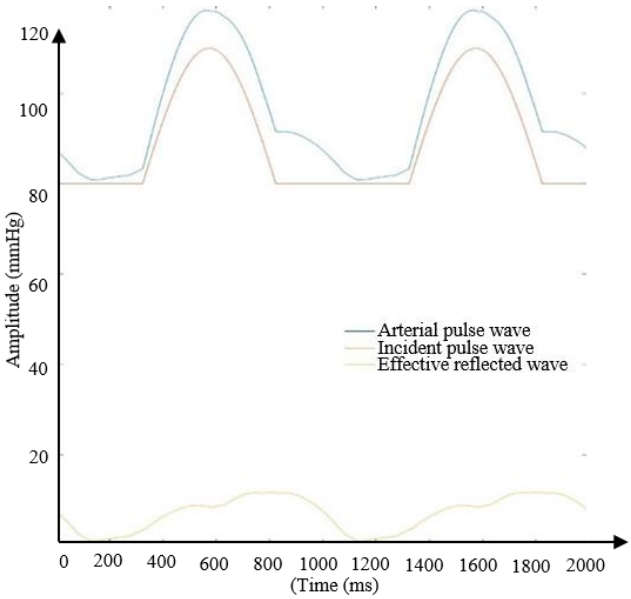

Figure 8. Tree representation constructed from arterial scheme in Fig. 7

Here, as in Fig. 8, we have $A(R_E) \approx 0.5 \times A(P_i)$. We further also observe a pronounced dicrotic notch. Importantly, though, and in contrast to Fig. 8, we have a much greater pulse wave amplification effect, augmenting systole to near 120. Thus, we see that using *in-vivo* parameters gives a more realistic blood pulse pressure waveform.

IV. Conclusion

The advantages of using the incredibly intuitive geometric tree representation in modeling blood pulse pressure wave propagation has the following advantages:

1. Representation of the full arterial system.
2. Simultaneous storage of "arterial geography" as well as propagation history.
3. Because the tree itself is a data structure, reflected wave computation can be done via recursive tree algorithms rather than via algorithms on data structures to which propagation history is transferred.
4. Inter-branching impedance mismatches can also be accommodated by this model, since such impedance mismatches are nothing more than reflection sites which can be represented by additional nodes in the tree structure.

In this paper, we qualitatively validate this graphical tree representation, showing that using *in-vivo* arterial segment measurements both a realistic waveform and pulse wave amplification effect are observed. However, there are still imperfections that must be dealt with. Most notably, this model, along with its counterparts, relies on reflection and transmission coefficient information to already be on hand. These coefficients, however, are determined by the unique physiological parameters, such as arterial distensibility, of individual patients. The challenge, then, is to model the interaction of these measurable parameters in such a way to produce the reflection and transmission coefficients that propagation histories are comprised of.

References

[1] P. Segers et al., "Limitations and pitfalls of non-invasive measurement of arterial pressure wave reflections and pulse wave velocity," *Artery Res.*, vol. 3, no. 2, pp. 79-88, 2009.

[2] A. Swillens and P. Segers, "Assessment of arterial pressure wave reflection: Methodological considerations," *Artery Res.*, vol. 2, no. 4, pp. 122-131, 2008.

[3] A. Cornet, "Mathematical modelling of cardiac pulse wave reflections due to arterial irregularities," *Math. Biosci. Eng.*, vol. 15, no. 5, pp. 1055-1076, 2018.

[4] J. Alastruey, K. Parker and S. Sherwin, "Arterial pulse wave hemodynamics," *11th Int. Conf. Pressure Surges*, 2012, pp. 401-443.

[5] P. Segers, J. Mynard, L. Taelman, S. Vermeersch and A. Swillens, "Wave reflection: myth or reality?," *Artery Res.*, vol. 6, no. 1, pp. 7-11, 2012.

[6] P. Reymond, F. Merenda, F. Perren, D. Rüfenacht and N. Stergiopulos, "Validation of a one-dimensional model of the systemic arterial tree," *Am. J. Physiol. Heart Circ. Physiol.*, vol. 297, no. 1, pp. H208-H222, 2009.